

## Short Note

# First evidence for the two-proton decay of $^{45}\text{Fe}$

M. Pfützner<sup>1,a</sup>, E. Badura<sup>2</sup>, C. Bingham<sup>3</sup>, B. Blank<sup>4</sup>, M. Chartier<sup>5</sup>, H. Geissel<sup>2</sup>, J. Giovinazzo<sup>4</sup>, L.V. Grigorenko<sup>2</sup>, R. Grzywacz<sup>1</sup>, M. Hellström<sup>2</sup>, Z. Janas<sup>1</sup>, J. Kurcewicz<sup>1</sup>, A.S. Lalleman<sup>4</sup>, C. Mazzocchi<sup>2</sup>, I. Mukha<sup>2</sup>, G. Münzenberg<sup>2</sup>, C. Plettner<sup>2</sup>, E. Roeckl<sup>2</sup>, K.P. Rykaczewski<sup>6,1</sup>, K. Schmidt<sup>7</sup>, R.S. Simon<sup>2</sup>, M. Stanoiu<sup>8</sup>, and J.-C. Thomas<sup>4</sup>

<sup>1</sup> Institute of Experimental Physics, Warsaw University, PL-00-681 Warszawa, Poland

<sup>2</sup> GSI, Planckstrasse 1, D-64291 Darmstadt, Germany

<sup>3</sup> Department of Physics and Astronomy, University of Tennessee, Knoxville 37996 TN, USA

<sup>4</sup> CEN Bordeaux-Gradignan, F-33175 Gradignan Cedex, France

<sup>5</sup> Oliver Lodge Laboratory, Department of Physics, University of Liverpool, Liverpool, L69 3BX, UK

<sup>6</sup> Physics Division, ORNL, Oak Ridge, TN 37831-6371, USA

<sup>7</sup> Department of Physics and Astronomy, University of Edinburgh, Edinburgh EH9 3JZ, UK

<sup>8</sup> GANIL, BP 5027, F-14021 Caen Cedex, France

Received: 17 May 2002

Communicated by J. Äystö

**Abstract.** Decays of five  $^{45}\text{Fe}$  atoms have been observed at the fragment separator of GSI. Whereas one event is consistent with the  $\beta$ -decay of  $^{45}\text{Fe}$  accompanied by the emission of a 10 MeV proton, four decays are consistent with the emission of particle(s) of total energy  $1.1 \pm 0.1$  MeV. This observation represents the first evidence for two-proton ground-state radioactivity, a decay mode predicted for  $^{45}\text{Fe}$ . The time distribution of the observed decay events corresponds to a half-life of  $3.2_{-1.0}^{+2.6}$  ms.

**PACS.** 21.10.Tg Lifetimes – 23.50.+z Decay by proton emission – 29.30.Ep Charged-particle spectroscopy

## 1 Introduction

Two-proton (2p) radioactivity was discussed theoretically for the first time by Goldansky in the early sixties [1]. This process, resulting in a simultaneous emission of two protons, can be described either via a  $^2\text{He}$  (diproton) particle subsequently splitting into two protons or as a genuine three-body decay which was reported, *e.g.*, for the cases of the broad resonance states of  $^6\text{Be}$  [2] and  $^{12}\text{O}$  [3]. Simultaneous emission of two protons has also been observed from the decay of 6.15 MeV,  $I^\pi = 1^-$  level in  $^{18}\text{Ne}$ , produced recently in the reaction  $^{17}\text{F} + \text{p}$  [4,5]. While the above cases involve *broad* states, two-proton radioactivity, *i.e.* the 2p emission from a *narrow* nuclear ground state, is energetically possible only for extremely proton-rich nuclei. Shell model calculations [6,7] and Coulomb-energy systematics [8] have identified  $^{45}\text{Fe}$  as one of the prime candidates for this decay mode, with  $Q$ -values of about 1 and 19 MeV being predicted for its 2p and EC decay, respectively.

$^{45}\text{Fe}$  was observed for the first time by Blank *et al.* [9] at the fragment separator (FRS) of GSI Darmstadt. Three events of this exotic  $T_z = -7/2$  nucleus were identified

following the fragmentation of a 600 MeV/nucleon  $^{58}\text{Ni}$  beam on a beryllium target. Apart from a lower limit of the half-life, deduced from the flight time through the separator, no decay properties could be determined. The next attempt to investigate nuclei around  $^{45}\text{Fe}$  was undertaken at the GANIL LISE3 separator, where quasifragmentation of a  $^{58}\text{Ni}$  beam on a nickel target was applied [10]. Among the results, the existence of  $^{45}\text{Fe}$  was confirmed with better statistics, doubly magic  $^{48}\text{Ni}$  was identified for the first time [10], and the decay properties of the nuclei in this region were measured [11]. In particular, decay events following the implantation of  $^{45}\text{Fe}$  were detected, and its half-life was determined to be  $6_{-3}^{+17}$  ms. However, although all ions of interest were implanted in a 300  $\mu\text{m}$  thick silicon detector, decay events were triggered *only* by those  $\beta$ -particles which left this implantation detector and were registered in the neighboring silicon detectors. Thus, events corresponding to implanted  $^{45}\text{Fe}$  nuclei decaying by the emission of two protons, with the expected total energy release of the order of 1 MeV [6–8], would not trigger the acquisition system. In such case, the observed decays and the estimated half-life correspond to the daughter nucleus  $^{43}\text{Cr}$  rather than to  $^{45}\text{Fe}$ .

<sup>a</sup> e-mail: pfutzner@mimuw.edu.pl

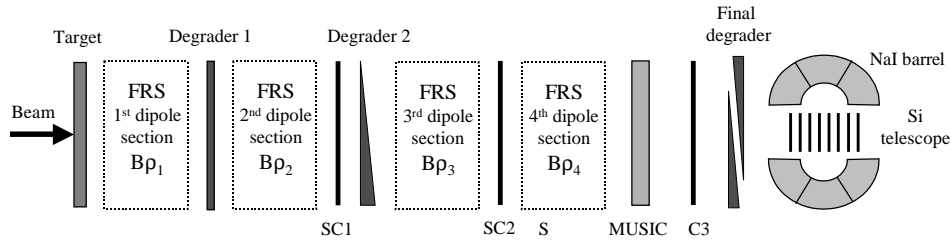


**Fig. 1.** Schematic drawing of the main FRS components and the spectroscopy setup. See text for details.

In order to clarify the situation as to the decay modes of  $^{45}\text{Fe}$ , a new experiment was performed at the FRS, the results of which are reported here. Since the  $2p$  decay of  $^{45}\text{Fe}$  may lead to a half-life as short as a few microseconds, a dedicated experimental setup was implemented to achieve sensitivity to decay times in a broad range from a few microseconds to several milliseconds. The setup included, *e.g.*, newly developed preamplifiers, equipped with a fast-reset function, and digital gamma finder (DGF-4C) modules [12]. Digital processing of charged-particle signals from silicon (Si) detectors by means of the DGF-based acquisition system had previously been successfully applied to study one-proton radioactivity. In particular, decay events of  $3\ \mu\text{s}$   $^{145}\text{Tm}$  were observed starting from about 500 ns after the implantation of these  $\approx 15$  MeV ions [13,14]. In the present experiment implantation signals of  $^{45}\text{Fe}$  were at the 1 GeV level, requiring a novel approach to the detection technique. A detailed description and, in particular, the demonstration of the sensitivity to decays within microseconds after heavy-ion implantation, will be published separately [15,16].

## 2 Experimental technique

The isotopes of interest were produced by projectile fragmentation between a 650 MeV/nucleon  $^{58}\text{Ni}$  beam, delivered by the SIS synchrotron, and a 4 g/cm<sup>2</sup> thick beryllium target located at the entrance of the FRS [17]. The average intensity of the primary beam was  $4 \times 10^9$  ions per spill while the length and the repetition period of the spill were 2 s and 7.6 s, respectively. In order to reduce the rate of contaminant ions passing through the FRS, a homogeneous aluminum degrader of 3.2 g/cm<sup>2</sup> thickness was placed at the first focal plane of the FRS, in addition to the standard wedge-shaped aluminum degrader mounted at the intermediate focal plane (see fig. 1). The thickness of the latter was set to 3.6 g/cm<sup>2</sup> at the optical axis, and the angle of the wedge was selected by the condition that the whole ion optical system be achromatic.

Each ion reaching the final focal plane of the FRS was identified in-flight using a detector setup consisting of 3 plastic scintillators (SC1, SC2 and SC3) and a four-fold ionization chamber (MUSIC), as shown in fig. 1. The MUSIC detector provided energy loss ( $\Delta E$ ) information from which the atomic number  $Z$  could be determined. The scintillators were mounted at the second, the third, and the final focal planes, respectively, and served for both

position and time-of-flight (TOF) measurements. The position information was determined from the time difference between signals read out from the right and left side of each scintillator. These observables, together with the magnetic-field values of the FRS dipoles, allowed the determination of the mass-to-charge ratio  $A/q$  for each ion. (Since all investigated nuclei were transmitted through the separator as fully stripped ions,  $q = Z$ .)

After passing the last identification detector, the ions were slowed down in an aluminum degrader of variable thickness and implanted into a telescope consisting of 8 Si detectors, each 60 mm in diameter and 300  $\mu\text{m}$  thick. The telescope was mounted inside a NaI(Tl) “split barrel” composed of 6 crystals. The NaI crystals were 30 cm long and the outer and the inner diameters of the barrel were 40 cm and 8 cm, respectively [18].

Two sets of preamplifiers were used to process the Si detector signals. One consisted of standard charge-sensitive low-gain preamplifiers providing information on the heavy-ion progressing through the telescope and allowing the determination of the detector in which the ion was stopped. Since the energies released during the stopping process reached values up to 1 GeV, a second set of high-gain preamplifiers was needed to detect the much smaller ( $\approx 1$  MeV) decay signals expected to follow within a very short time of the implantation. For this purpose standard preamplifiers cannot be applied, as they would be saturated for several milliseconds by the large heavy-ion-induced pulse. To overcome this difficulty, a new type of preamplifier was constructed incorporating a special fast-reset function which allows to block the input circuit by an external logical pulse. Such pulses, generated each time a heavy ion passed the first silicon detector, were used to block the seven fast-reset preamplifiers connected to detectors nos. 2–8 for 2  $\mu\text{s}$ . In this way, decay signals of  $\approx 1$  MeV energy can be detected already a few microseconds after the implantation of a heavy ion [15].

Two independent acquisition systems were used to process and store the data. The first one was based on DGF-4C modules [12]. The preamplifier outputs (4 from the MUSIC detector, 8 from the low-gain and 7 from the fast-reset Si signals) as well as 6 photomultiplier outputs from the NaI barrel were connected directly to the DGF-4C inputs. The photomultiplier signals from SC1, SC2 and SC3 were preprocessed by analog electronics, and the time differences required for the position and TOF measurements were determined by using time-to-amplitude converters (TAC) before passing the TAC outputs to the DGF-4C

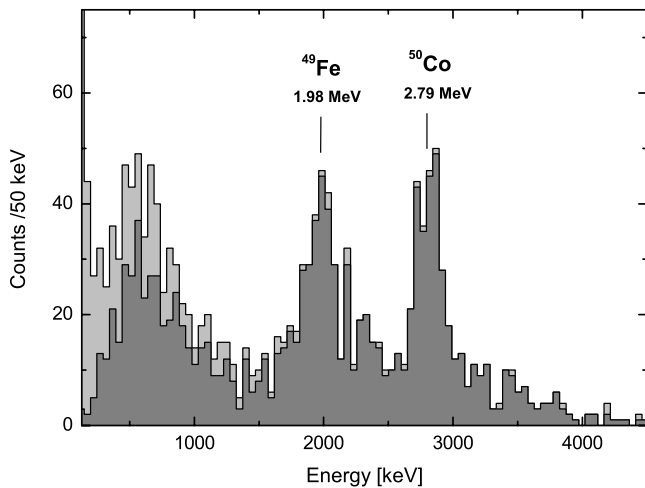


**Fig. 2.** Singles  $\beta p$  spectrum, obtained by implanting both  $^{49}\text{Fe}$  and  $^{50}\text{Co}$  in the Si telescope and summing events from Si detectors 2–7. The dark grey area indicates events coincident with signals from the NaI barrel.

modules. The function of the DGF-4C module consists of digitizing each input signal with a 25 ns step, determination of amplitude and time stamp by an on-board digital signal processor, and subsequent storage in the internal memory buffer.

In order to prevent numerous “contaminant” ions with  $A/q \gtrsim 2$  from triggering the DGF data acquisition, the data collection was only triggered when a heavy ion was detected in the first Si detector and the corresponding TOF value was above the limit adjusted to select ions with a low  $A/q$  ratio (see fig. 3 in the following). Once the system was triggered, signals from all detectors were accepted and processed for 10 ms. In this way all information on heavy ions, decays and  $\gamma$  events happening within 10 ms after the arrival of a triggering ion were collected *dead time free* in the DGF-4C memory buffers. Their contents was read out afterwards and stored on a magnetic tape.

In the second data acquisition system, independent of the first one, all signals were processed by standard analog electronics. This system was triggered by SC3 signals, thus practically by every heavy ion reaching the final focus. (During the experiment, after 3 ions of  $^{45}\text{Fe}$  had been identified, the system was modified also to allow decay signals from the Si telescope to trigger the acquisition.) All data accumulated by the ADC and TDC modules within a few microseconds following the trigger were read out and stored on a second magnetic tape. This system, which allowed constant monitoring of all ion species transmitted through the FRS, was used primarily for tuning the FRS, checking its stability, and adjusting the implantation of selected ions. It suffered, however, from a large dead time of about 40% at the typical rate of 1000 ions/s at the final focus.

The whole detection system was calibrated using low-intensity primary beam degraded to different energies as well as by implanting the known  $\beta$ -delayed proton ( $\beta p$ ) emitters  $^{49}\text{Fe}$  and  $^{50}\text{Co}$  [19] in the Si telescope. The energy

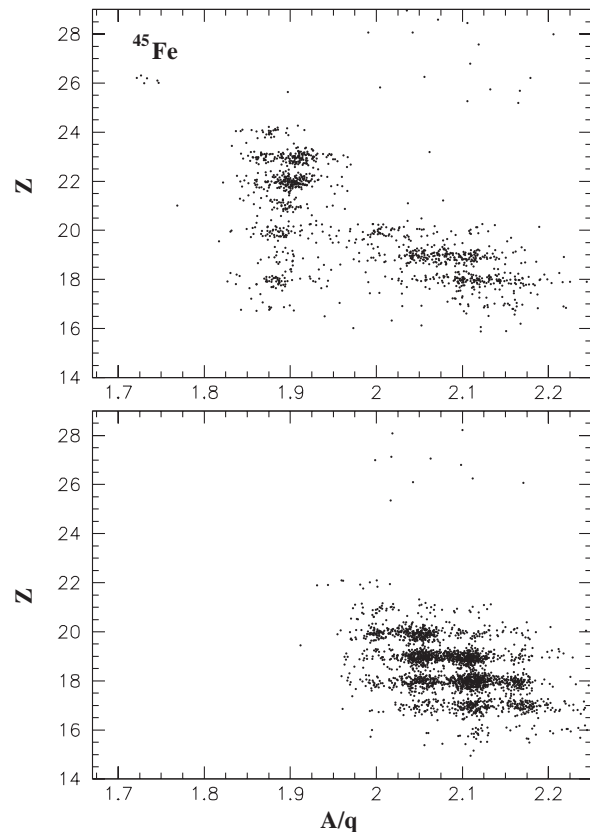


**Fig. 3.** Atomic number  $Z$  versus mass-over-charge ratio  $A/q$  (determined from the TOF between SC2 and SC3) of those ions which entered the Si telescope. In the upper panel only ions which triggered the DGF acquisition system are indicated. The lower panel shows all ions which were detected in the 10 ms periods following each start of the DGF system.

resolution (FWHM) for the 1.98 MeV proton line from  $^{49}\text{Fe}$  was found to be about 250 keV. Since the last Si detector (8) was not well calibrated, it was disregarded in the following analysis. The corresponding spectrum of protons summed over the Si detectors 2–7 is shown in fig. 2. A comparison of this spectrum to that obtained in coincidence with signals from the NaI barrel yields a rejection efficiency of 93% over the  $\beta p$  energy range 0.9–4 MeV (see fig. 2).

### 3 Results

For the  $^{45}\text{Fe}$  measurement, the magnetic rigidities of the four FRS sections were set to 6.438, 5.571, 4.846 and 4.768 Tm, respectively. The measurement lasted about 6 days with a total counting time of 8120 min. On average, the SC1 and SC3 rates were approximately  $20000 \text{ s}^{-1}$  and  $1500 \text{ s}^{-1}$ , respectively. About 200 ions/s entered the Si telescope. In total the DGF acquisition system was triggered 2115 times, corresponding to an average period of 3.8 min between registered events. The identification plot of those ions that started this acquisition is shown in the upper panel of fig. 3. Six events of  $^{45}\text{Fe}$  can be clearly

**Table 1.** Implantation detector, decay energy and decay time recorded for each of the six  $^{45}\text{Fe}$  decays observed (events are ordered chronologically). See text for details.

Event	Detector	$E$ (keV)	$T$ (ms)
1	4	$1000 \pm 120$	0.644
2	3	$990 \pm 130$	5.276
3	5	$10010 \pm 100$	3.395
4	5	–	–
5	2	$1150 \pm 100$	1.196
6	2	$1200 \pm 100$	12.617

seen. The effect of the TOF condition imposed to select ions with a low  $A/q$  ratio is evident: albeit some contaminant ions with  $A/q > 1.95$  did start the acquisition, these were suppressed by a large factor. The lower panel shows ions recorded by the DGF system to have entered the Si telescope during the 10 ms period following each start, as described in sect. 2. About 4000 such ions were detected during the total counting time of 21 s ( $2115 \times 10$  ms), in agreement with the measured rate of 200 ions/s hitting the Si telescope. The most abundant of these contaminant ions are  $^{40-43}\text{Ca}$ ,  $^{39-40}\text{K}$ ,  $^{37-39}\text{Ar}$  and  $^{35-37}\text{Cl}$  which represent stable or very long-lived isotopes, though a number of  $\beta^+$ -decaying isotopes with half-lives ranging from 50 ms ( $^{45}\text{Cr}$ ) to 3.9 h ( $^{43}\text{Sc}$ ) are also present.

The signals delivered by the low-gain preamplifiers allowed to determine in which Si detector each of the  $^{45}\text{Fe}$  ions was stopped. Based on this information, decay signals originating from the same detector were inspected. The results of this search are compiled in table 1.

The fast-reset preamplifier connected to Si detector 5 suffered intermittently from a large baseline shift in the output signal. Unfortunately, the fourth event occurred during such a malfunction and no decay signals following this event could be registered. In the remaining five cases, an energy release was observed which was assigned to the decay of implanted  $^{45}\text{Fe}$  ions. The decay signal of event 5 was registered by both acquisition systems. The decay following event 6 was detected only by the standard acquisition, as it occurred 12.6 ms after the implantation and thus was outside of the 10 ms sensitivity window of the DGF system.

In one case (event 3) a decay energy of  $\approx 10$  MeV was found as the sum of coincident contributions of 3.89 MeV from detector 4 and 6.12 MeV from detector 5. Moreover, a coincident  $\gamma$ -ray of about 900 keV was detected in one of the NaI crystals. In view of the large  $Q_{\text{EC}}$  of 19 MeV predicted [6–8] for  $^{45}\text{Fe}$ , this observation is consistent with the  $\beta^+$ -decay of this nucleus, involving a  $\beta\text{p}$  event. An alternative assignment would be the  $\beta^+$ -decay of  $^{43}\text{Cr}$ , the 2p decay daughter of  $^{45}\text{Fe}$ . In order to support such tentative interpretations, improved data are clearly needed. In all four other cases, however, a completely different pattern is observed: the energy of about 1 MeV is released in the Si detector where the ion was stopped, with no other signal in coincidence. This pattern is expected if  $^{45}\text{Fe}$  decays by the emission of two protons from the ground state.

Because the number of observed decay events is so low, we have carefully examined the possibility that the observed signals originate from the decay of other ions or from random background, as discussed in the following.

Two sources for low-energy signals that are observed in the Si detectors can be considered: background and true radioactivity. The background originates in light particles produced in secondary reactions induced in the different material layers of the FRS by transmitted heavy ions. These events can be recognized by two characteristic features: a) a low-energy decay-like signal is coincident with signals delivered by heavy-ion identification detectors (SC1, SC2, SC3, MUSIC), and/or b) several Si detectors fire simultaneously. To suppress this unwanted background, only signals from the Si telescope which are in anti-coincidence with all heavy-ion detectors, and which represent either single hits (one Si detector fired) or the simultaneous firing of two neighboring Si detectors, should be selected. (The latter may occur in case of  $\beta\text{p}$  emission from an ion implanted close to the detector surface.) All decays attributed to  $^{45}\text{Fe}$  (table 1) fulfill this condition.

Potentially, the remaining events could originate from the decay of other ions that had been implanted into the telescope rather than from the radioactive decay of the implanted  $^{45}\text{Fe}$  ions. However, the complete 10 ms “history” of each event provided by the DGF system allowed to check if any other ions were implanted in the Si telescope between the  $^{45}\text{Fe}$  and the decay. Indeed, it was found that in the case of events 2, 3, 5, and 6 some contaminant ions were detected in the telescope before a decay event occurred. They represent, however, either stable or very long-lived species, and all but one were stopped in a different detector than the triggering  $^{45}\text{Fe}$  ion. Only in one case (event 2) a second ion was possibly stopped in the same detector as the  $^{45}\text{Fe}$  during the 10 ms interval, but it was identified as a stable isotope ( $^{38}\text{Ar}$ ). Thus, we conclude that these contaminant ions could in no case be responsible for the observed decay signals.

To check if other ions triggering the DGF acquisition were correlated with any decay signals, all decay events occurring in the same detector were investigated for each stopped ion. Figure 4 compares the results of this procedure for the 6 events associated with  $^{45}\text{Fe}$  (upper part) and for 664 other ions (lower part). While 5 decay events are correlated with  $^{45}\text{Fe}$ , the lower spectrum is empty above 800 keV. Apart from a few low-energy events attributed to noise, there are two counts around 500 keV which were found to be correlated with implanted  $^{44}\text{V}$  nuclei. Since about 60 ions of  $^{44}\text{V}$  ( $T_{1/2} = 150$  ms) were stopped, the number of observed decays agrees with what is expected within a period of 10 ms. This represents an upper limit of this background type, as the probability to detect decays of other triggering contaminants is even smaller due to their lower rates and/or longer lifetimes.

A potentially more dangerous source of accidental implantation decay coincidences are the less exotic contaminant ions, identified in the lower part of fig. 3. These were implanted in the telescope at a constant total rate of about 200 ions/s, and since they include isotopes with

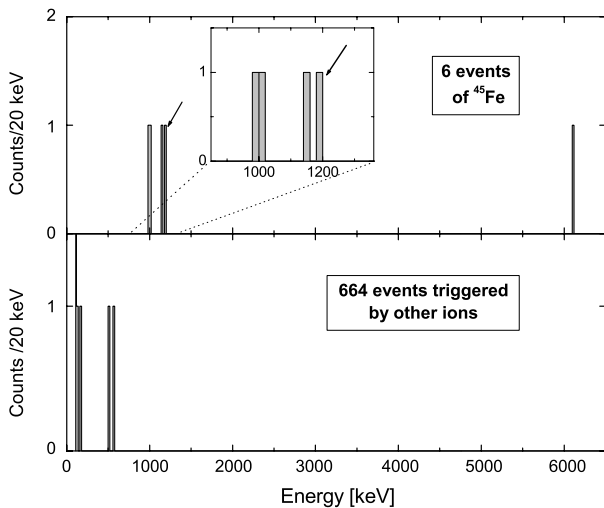


**Fig. 4.** Spectra of all decay events registered in the same detector in which a triggering heavy ion was stopped. The upper part corresponds to 6 events of  $^{45}\text{Fe}$ , while the lower part shows the results obtained for 664 other ions. Detectors 2–7 were taken into account. The count detected only in the standard acquisition (event 6) is marked with an arrow.

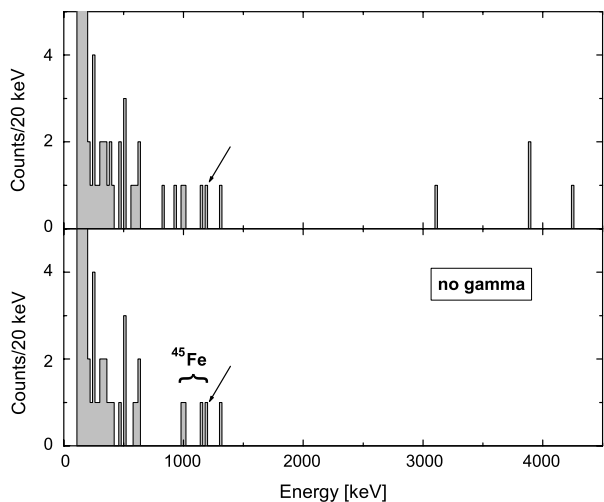


**Fig. 5.** Singles spectra of all decay events in detectors 2–7 recorded by the DGF system during the whole run. The lower spectrum was accumulated with the condition that no signal is detected in the NaI barrel in coincidence. Event 6, detected only in the standard acquisition, is marked with an arrow.

half-lives between seconds and hours, some of them may randomly decay within the 10 ms observation period started by a different ion. To estimate this contribution to the background, singles spectra including all decay events registered during the whole run (2115 triggers) were investigated. The results are plotted in fig. 5. Several counts are observed in the region above 700 keV (upper spectrum) but many of them disappear when an anti-coincidence with the NaI barrel is required (lower spectrum). Among the remaining 5 counts, 4 represent signals correlated to  $^{45}\text{Fe}$  and only one count is left (at 1300 keV) which has to be considered as random background and

which has the same properties as counts attributed to the decay of  $^{45}\text{Fe}$ . It follows that the probability to detect such random events during a 10 ms observation period is  $\approx 10^{-3}$ . Thus, it is very unlikely that all four  $\approx 1$  MeV signals following the implantation of  $^{45}\text{Fe}$  represent this sort of random background.

Finally, a statistical test, proposed by Schmidt [20], can be applied to verify that measured decay times are consistent with the assumption that they originate from the radioactive decay of a single species (single half-life). The test is based on the observation that the decay curve in a logarithmic time scale has a universal shape independent of the half-life. The expected standard deviation of the  $\ln t_i$ -values, where  $t_i$  is the decay time of the  $i$ -th event, for the 5 data points is equal to 1.06 and should on a 90% confidence level be found between 0.41 and 1.90 [20]. The standard deviation of the measured decay times (table 1) is equal to 1.04, very close to the expected value.

We, therefore, conclude that the decay signals observed to be correlated with implanted  $^{45}\text{Fe}$  ions do represent the decay of this nuclide. The half-life estimated by the maximum-likelihood method [21] for the 5 data points is  $T_{1/2} = 3.2^{+2.6}_{-1.0}$  ms. Our data thus suggest that  $^{45}\text{Fe}$  decays predominantly ( $\approx 80\%$ ) by the emission of charged particle(s) with a total energy of  $1.1 \pm 0.1$  MeV.

## 4 Discussion

The non-observation of  $\gamma$ -rays coincident with the dominant decay mode of  $^{45}\text{Fe}$  is not compatible with a  $\beta$ -decay scenario. In the case of  $\beta p$  emission to the ground state of  $^{44}\text{Cr}$ , the expected  $\beta p$  energy is larger than 8 MeV [7, 11] and the proton would be accompanied by two 511 keV annihilation photons. If the transition, instead, proceeds to excited states in the final nucleus, the  $\beta p$  energy would be smaller, but at least one additional  $\gamma$ -ray would be emitted. Based on the NaI barrel  $\gamma$ -ray detection efficiency estimates, it is indeed very improbable that the  $\gamma$ -ray would escape detection in all four instances of  $^{45}\text{Fe}$  decay observed with the energy of the emitted particle(s) having such a similar value. The corresponding escape probabilities for  $\beta$ -delayed  $\gamma$ -rays of multiplicity 2 and 3 amount to  $10^{-4}$  and  $10^{-6}$ , respectively.

On the other hand, the observed decay pattern is in good agreement with the prediction for the two-proton decay mode [6–8]. While the  $Q$ -value for one-proton emission from the  $^{45}\text{Fe}$  ground state is expected to be close to zero or negative, the estimated  $Q$ -values for 2p emission ( $Q_{2p}$ ) are  $(1.154 \pm 0.094)$  MeV [6],  $(1.279 \pm 0.181)$  MeV [7], and  $(1.218 \pm 0.049)$  MeV [8].

Calculations of the half-life based on the two-body  $R$ -matrix formalism, which treats the two protons as a  $^2\text{He}$  (diproton) particle with zero angular momentum, and assuming a spectroscopic factor  $\theta^2 = 1$ , yield broad intervals reflecting the inaccuracies in the transition energy:  $(2 \mu\text{s} - 300 \mu\text{s})$  [6] and  $(10 \text{ ns} - 100 \mu\text{s})$  [7]. The spectroscopic factors calculated by these authors would increase these limits by a factor of about 5. However, as pointed out by

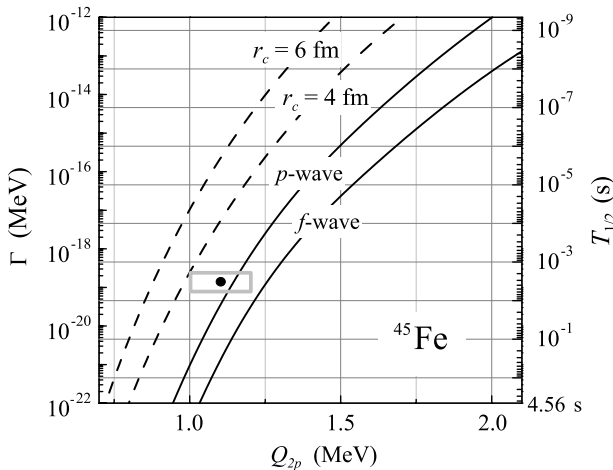


**Fig. 6.** Results of different theoretical estimates of the partial half-life for the ground-state 2p decay of  $^{45}\text{Fe}$ . The experimental value from this work is indicated by the box. See text for details.

Grigorenko *et al.* [22,23], who have developed a rigorous three-body model to study the two-proton radioactivity, the diproton approximation may overestimate the emission rate by two to three orders of magnitude and should be considered rather as the lower limit for the half-life.

Figure 6 shows the results of various theoretical estimates. The solid lines represent calculations within a three-body approach, assuming either a pure  $p^2$  or  $f^2$  configuration for the two-valence protons to illustrate the influence of the spectroscopic factor. For comparison, two predictions from the diproton model (dashed lines) are shown, corresponding to channel radii  $r_c$  of 4 fm [22] and 6 fm, respectively. The experimental result,  $T_{1/2} = 3.2_{-1.0}^{+2.6}$  ms, does not exceed the diproton lower limit, even for very low channel radii. It is also in good agreement with the three-body model prediction of  $T_{1/2} = 13$  ms, obtained assuming  $Q_{2p} = 1.1$  MeV.

The emission of two protons from  $^{45}\text{Fe}$  populates  $^{43}\text{Cr}$  which subsequently beta-decays with the half-life  $T_{1/2} = 21.6 \pm 0.7$  ms [11]. The DGF system did not register any such daughter decays. We estimate the probabilities to observe the decay of  $^{43}\text{Cr}$  within the remaining part of the 10 ms period after the decay of  $^{45}\text{Fe}$  were 26%, 14%, and 25% for events 1, 2, and 5, respectively. Thus, the probability of non-observation of the daughter decay in these three events amounts to about 48%. The daughter decays of events 5 and 6 could have been detected by the standard acquisition. Only one candidate was found, 16.8 ms after the decay of  $^{45}\text{Fe}$  event number 6. The non-observation of a daughter decay associated with event 5 is likely explained by the large dead time of the standard acquisition.

According to our interpretation, the events attributed to the  $\beta$ -decay of  $^{45}\text{Fe}$  by Giovinazzo *et al.* [11] instead represent the decay of  $^{43}\text{Cr}$ . Indeed, the half-life value and decay energy spectrum correlated with  $^{45}\text{Fe}$  (fig. 14 of ref. [11]) does not contradict the corresponding data obtained for  $^{43}\text{Cr}$  (fig. 4 of ref. [11]).

## 5 Summary

To summarize, we have investigated the decay of  $^{45}\text{Fe}$ . Six atoms of this nuclide, produced by the fragmentation of a 650 MeV/nucleon  $^{58}\text{Ni}$  beam, separated by the FRS and identified unambiguously in-flight, were implanted in a telescope composed of 8 Si detectors of 300  $\mu\text{m}$  thickness. For five of the implanted  $^{45}\text{Fe}$  atoms, decay signals were recorded. One decay event is consistent with a  $\beta$ -decay scenario. In the remaining four cases, an energy release of  $1.1 \pm 0.1$  MeV was observed. The half-life of  $^{45}\text{Fe}$  was estimated to be  $T_{1/2} = 3.2_{-1.0}^{+2.6}$  ms.

This work, made possible by applying newly developed fast-reset preamplifier modules in conjunction with digital pulse-shape analysis of the corresponding charged-particle detector signals, represents the first evidence for the ground-state two-proton radioactivity of  $^{45}\text{Fe}$ . This assignment is strongly supported by the absence of coincidences with  $\beta$ -delayed  $\gamma$ -rays. Additional measurements providing data with better statistics and improved energy resolution are clearly needed to confirm this result. In addition, future investigations should include tracking of the emitted particles to distinguish between three-body and two-body decay processes.

It should be noted that after the present work was completed, our results were independently confirmed by the analysis of data obtained at GANIL [24].

We are grateful to K.-H. Behr, A. Brünle and W. Hüller for the excellent technical support in the preparation phase and during the experiment. Efforts of the GSI synchrotron staff to provide a high-intensity primary beam are also acknowledged. This work was partially supported by the EC under contract HPRI-CT-1999-50017 and by the U.S. DOE through contract DE-FG02-96ER40983 (University of Tennessee). ORNL is managed by UT-Battelle, LLC, for the U.S. DOE under contract DE-AC05-00OR22725.

## References

1. V.I. Goldansky, Nucl. Phys. **19**, 482 (1960).
2. O.V. Bochkarev *et al.*, Sov. J. Nucl. Phys. **55**, 955 (1992).
3. R.A. Kryger *et al.*, Phys. Rev. Lett. **74**, 860 (1995).
4. J. Gomez del Campo *et al.*, Phys. Rev. Lett. **86**, 43 (2001).
5. L.V. Grigorenko *et al.*, Phys. Rev. C **65**, 044612 (2002).
6. B.A. Brown, Phys. Rev. C **43**, (1991) R1513.
7. E. Ormand, Phys. Rev. C **53**, 214 (1996).
8. B.J. Cole, Phys. Rev. C **54**, 1240 (1996).
9. B. Blank *et al.*, Phys. Rev. Lett. **77**, 2893 (1996).
10. B. Blank *et al.*, Phys. Rev. Lett. **84**, 1116 (2000).
11. J. Giovinazzo *et al.*, Eur. Phys. J. A **10**, 73 (2001).
12. B. Hubbard-Nelson, M. Momayezi, W.K. Warburton, Nucl. Instrum. Methods Phys. Res. A **422**, 411 (1999).
13. R. Grzywacz *et al.*, to be published in *Proceedings of the Third International Conference on Exotic Nuclei and Atomic Masses (ENAM2001)*, Hämeenlinna, Finland, 2001 (Springer, 2002).
14. K.P. Rykaczewski *et al.*, Nucl. Phys. A **682**, 270c (2001).

15. M. Pfützner *et al.*, to be published in Nucl. Instrum. Methods Phys. Res. A.
16. R. Grzywacz, in *Proceedings of the 14th International Conference on Electromagnetic Isotope Separators and Techniques Related to their Applications (EMIS-14), May 6-10, 2002, Victoria, Canada*, to be published in Nucl. Instrum. Methods Phys. Res. B.
17. H. Geissel *et al.*, Nucl. Instrum. Methods Phys. Res. B **70**, 286 (1992).
18. H. Keller *et al.*, Nucl. Instrum. Methods Phys. Res. A **300**, 67 (1991).
19. L. Faux *et al.*, Nucl. Phys. A **602**, 167 (1996).
20. K.H. Schmidt, Eur. Phys. J. A **8**, 141 (2000).
21. K.H. Schmidt *et al.*, Z. Phys. A **316**, 19 (1984).
22. L.V. Grigorenko *et al.*, Phys. Rev. C **64**, 054002 (2001).
23. L.V. Grigorenko *et al.*, Phys. Rev. Lett. **85**, 22 (2000).
24. J. Giovinazzo *et al.*, submitted to Phys. Rev. Lett.